Journal of Hazardous Materials 205–206 (2012) 32–39

Contents lists available at SciVerse ScienceDirect

Journal of Hazardous Materials

journal homepage: www.elsevier.com/locate/jhazmat

Controlling pesticide release via structuring agropolymer and nanoclays based materials

Anne Chevillard*, Hélène Angellier-Coussy, Valérie Guillard, Nathalie Gontard, Emmanuelle Gastaldi

UMR IATE, Université Montpellier II, CC023, pl. E Bataillon, 34095 Montpellier Cedex, France

ARTICLE INFO

Article history:
Received 23 September 2011
Received in revised form
24 November 2011
Accepted 27 November 2011
Available online 8 December 2011

Keywords:
Wheat gluten
Montmorillonite
Nanocomposite
Pesticide controlled release
Modelling

ABSTRACT

The potential use of nanoclays for modulating transfer properties of active agents in bio-sourced polymers was explored. For this purpose, new pesticide formulations were designed by combining wheat gluten, ethofumesate (model pesticide) and three montmorillonites (MMT) using a bi-vis extrusion process. Controlled release properties, evaluated through release experiments in water, were discussed in relation to the material formulations and their resulting structure. Partition coefficients were calculated from experimental data and diffusivity values were identified with a Fick's second law mechanistic model. The effect of temperature on release pattern was also evaluated and the activation energy of diffusion was determined. Ethofumesate release was slowed down for all wheat gluten based-formulations as compared to the commercial product. This slow release effect was increased in the presence of hydrophobic MMTs, due to a higher affinity for ethofumesate than for wheat gluten. Contrarily, hydrophilic MMT, displaying a greater affinity for wheat gluten than for ethofumesate seemed ineffective to slow down its release despite the tortuous pathway achieved through a well-exfoliated structure. To conclude, the release mechanisms would be rather governed by pesticide/MMT interactions than MMT/polymer matrix in the case of a hydrophobic pesticide such as ethofumesate and a hydrophilic matrix such as wheat gluten.

1. Introduction

The extensive use of pesticides has enabled to significantly increase food production. Nevertheless, this has resulted in serious environmental pollution and ecological issues since a large amount of applied pesticides often never totally reaches its intended target due to their degradation, volatilisation and leaching [1,2]. Consequently, to compensate for the loss of effectiveness of conventional pesticide formulation, products are often applied in quantities greatly exceeding those actually required. To overcome these problems, controlled release formulations (CRF) are considered as a pertinent alternative. The principle of CRF is to gradually deliver the active substance over time with the aim of limiting the amount immediately available for transport and degradation processes. CRF also allow the extension of the substance activity, the reduction of residue amounts on food stuffs, savings in manpower and energy by reducing the number of applications required, as well as an increased safety for those applying pesticides [3–8].

Among the different strategies used to develop CRF, inorganic supports such as clays have been considered as suitable supports for the controlled release of pesticides [9–11]. Numerous works have been devoted to montmorillonites (MMT) because of their large availability, natural presence in soils, high specific surface area and ion-exchange capacity conferring them a good ability to adsorb/desorb pesticides. MMT surface reactivity can also be easily modified through organic cation exchange reactions to modulate their affinity to a targeted pesticide, which constitutes another huge advantage of developing efficient CRF. Many studies have demonstrated that clay/pesticide complexes can be considered as suitable pesticide carriers since they display slow release properties [6,12–14]. Nevertheless, clay/pesticide complexes have some limits since powders are not convenient to be spread on fields compared to liquid and solid formulations.

Organic matrices have also been regarded as pesticide carriers worthy of attention. Even if synthetic polymers (urea-formaldehyde resins, acrylic acid polymers, polyurethane...) can be used as carriers [15], bio-sourced polymers are often preferred to design CRF due to their biodegradability and non-ecotoxicity. Potential CRF based on bio-sourced matrices include chitosan [16,17], pectin [4], polylactic acid [18], starch [19,20], alginate [21], starch–alginate [4,22–24], alginate–gelatin [25,26], lignin and/or cellulose derivatives [27–30] and wheat gluten [31,32]. Among them, wheat gluten, a by-product of the starch industry, can be considered as a very suitable raw material due to good thermoplastic properties and processability by extrusion at temperatures as low as 60 °C [33], remarkable biodegradability [34,35], availability

* Corresponding author. Tel.: +33 467 144 235; fax: +33 467 144 990.
E-mail addresses: anne.chevillard@univ-montp2.fr, anne.chevillard@gmail.com (A. Chevillard), helene.coussy@univ-montp2.fr (H. Angellier-Coussy), guillard@univ-montp2.fr (V. Guillard), gontard@univ-montp2.fr (N. Gontard), egastald@univ-montp2.fr (E. Gastaldi).

0304-3894/$ – see front matter © 2011 Elsevier B.V. All rights reserved.
doi:10.1016/j.jhazmat.2011.11.093

in large quantities at a reasonable price (around 1.3 €/kg) and a high protein content (>75 wt%) whose variety of amino acids offers a large spectrum of chemical functionalities. Moreover, protein-based materials present a huge advantage for agricultural applications since contributing to the nitrogen crop nutrition owing to the significant amount of nitrogen (around 17 wt%) that would be ultimately released in soil at the end of the biodegradation process.

Even if a polymer matrix can be efficient to modulate pesticide release, this efficiency can be improved by combining clay fillers in its formulation. Several studies have already reported that interesting slow release properties could be brought by adding nanoclays in cellulose derivatives [36], chitosan [37] or alginate [4,7,38,39] matrices. This slow release behavior is often attributed to clay sorption properties even if the addition of nanoclays may also lead to an exfoliated nanocomposite structure, expected to modulate diffusion [40,41].

With such a CRF associating polymer and nanoclays, the bioavailability of the active substance in soil would result from concomitant complex phenomena including (i) its diffusion through the material, (ii) its desorption from the clay particles depending on its affinity for the fillers and (iii) the matrix biodegradation rate. Thus, a better knowledge of each mechanism contribution would enable to better control the release pattern of a pesticide.

The present study aims at exploring the potential use of nanoclays for modulating transfer properties of active agents in bio-sourced polymers with the objective to design new CRF for pesticides. Since MMT was expected to delay the pesticide delivery by controlling its diffusion via a tortuosity effect and/or its sorption on nanoclays, we propose to evaluate the respective contribution of each phenomenon. For this purpose, ethofumesate, selected as a model pesticide, was introduced in wheat gluten/MMT materials using a bi-vis extrusion process. Indeed, ethofumesate (a widely used herbicide) has been chosen as a model pesticide in this study since its hydrophobicity ($\log P = 2.7$) and molecular weight (286.3 g mol^{-1}) might be considered as representative of commonly used organic pesticides. Moreover, ethofumesate displays an aromatic moiety and a heterocycle, which are relatively common in organic pesticides structure. Three types of MMT, displaying contrasted affinity for both the wheat gluten matrix and the pesticide, were selected based on previous results showing that adsorption/desorption mechanisms of ethofumesate on these MMT were mainly governed by their polarity and chemical structure [14]. Release experiments were conducted in water to study the influence of the formulation on both pesticide diffusivity within the material and partition coefficient between the material and water. Furthermore, experiments have been performed at different temperatures and the corresponding activation energy for diffusion has been evaluated. Controlled release properties were discussed in relation to the structure of materials at different scales.

2. Materials and methods

2.1. Materials

Commercial vital wheat gluten (WG) was kindly supplied by Syral (Belgium) under the reference AMYGLUTEN 110. Its moisture and protein content was approximately 10% and 80%, respectively. Technical ethofumesate [5-benzofuranol, 2-ethoxy-2,3-dihydro-3,3-dimethyl-, methanesulfonate, (±)] 97% pure was a crystalline solid kindly supplied by Bayer Crop Science (France). Analytical ethofumesate (99.5% pure) was purchased from Sigma–Aldrich to compare with calibration standards. A commercial formulation of ethofumesate (Tramat® F) was provided by Bayer Crop Science (France). The molecular mass of ethofumesate was 286.3 g mol^{-1} and its solubility in water ranged from 44 to 57 mg L^{-1} depending on the pH.

Three types of commercial nanoclays were used as received: an unmodified sodium montmorillonite provided by Laviosa (Italy) under the reference HPS, and two organically modified montmorillonite (OMMT), Cloisite® 30B (Southern Clay, noted C30B) carrying a methyl, tallow, bis-2-hydroxyethyl alkylammonium salt and Dellite 72T (Laviosa, noted D72T) which is modified with a di-methyl, di-tallow alkylammonium salt. CEC (cation exchange capacity) values were 129, 93 and 108 meq. 100 g^{-1} for HPS, C30B and D72T, respectively. CEC (cation exchange capacity) values were 129, 93 and 108 meq. 100 g^{-1} for HPS, C30B and D72T, respectively. Further information on nanoclays (organic content, organic cation saturation, 3D models of organic cations, interlayer distance) are given in Chevillard et al. [14].

Chemicals, unless specified separately, were purchased from Sigma–Aldrich in pure analytic quality.

2.2. Preparation of wheat gluten-based materials

Extrusion was performed using a co-rotating twin screw extruder (Coperion, ZSK25, Stuttgart, Germany) connected to a computer interface and controller unit (Brabender, O.H.G., Duisburg, Germany). The barrel consisted of twelve zones, each zone being equipped with an independent temperature control and a die head constituted of two 5 mm diameter holes. The total length of the screw was 42D. The first and second heating zones were set at 40 °C and the other heating zones at 60 °C. The screw speed was set at 150 rpm. Wheat gluten, nanoclays and ethofumesate powders were fed using two distinct weight feeders (Brabender, Duisburg, Germany) leading to a cumulate powder feed rate of 4.5 kg h^{-1}. The amounts of nanoclays and ethofumesate have been adjusted in such a way to obtain a constant inorganic filler content of 5 wt% d.b. and a targeted content of ethofumesate of 0.2 wt% d.b. Water was fed with a weight pump (Movacolor, WL Sneek, Netherlands) at a flow rate of 2 kg h^{-1}. Immediately after extrusion, extrudates were cooled and air-dried in ambient conditions for approximately 30 min before being cut using a Scheer SGS 50E pelletizer (Scheer Reduction Engineering GmbH, Stuttgart, Germany). Cylindrical shaped granulates were allowed to dry in ambient room conditions until constant weight. The water content of the final granulates was 9 wt%. Samples were packed in hermetically sealed polyethylene bags and stored in a dark room at 4 °C until needed for the experiments.

2.3. Thermal stability of ethofumesate

The thermal stability of ethofumesate was investigated through thermogravimetric analysis (TGA) by using a Diamond TGA/DTA device from PerkinElmer (USA). Experiments were conducted on about 20 mg of dry sample from room temperature to 800 °C with a heating ramp of 10 °C min^{-1} and under air flow. The thermal degradation was characterized by three temperatures: (i) the temperature corresponding to the beginning of the degradation process, i.e., at which the absolute value of the first derivative of the weight loss became higher than 0.1%/°C (T_{onset}), (ii) the temperature at which the degradation rate was maximum (T_{peak}) and (iii) the temperature corresponding to the end of the degradation process, i.e., at which the absolute value of the first derivative of the weight loss became lower than 0.1%/°C (T_{offset}). Experiments were performed in duplicate.

2.4. Morphological characteristics and ethofumesate content of wheat gluten-based materials

For each formulation, the average thickness and diameter were determined from measurements performed on 30 granulates with

a digital calliper with an accuracy of ±0.01 mm. The average weight of granulates was measured on three groups of 30 granulates using a four-digit balance.

Ethofumesate content was evaluated after extraction, conducted as follows. Ground samples (1.00 g) were stirred for 5 min at 10,000 rpm with a high shear laboratory mixer (Silverson L4RT, England) at 25 °C into 20 mL of methanol. Solutions were firstly passed through 5 μm cellulose filters and then through 0.45 μm nylon filters before HPLC analyses (Section 2.6).

2.5. Structure characterization of wheat gluten-based materials

2.5.1. Cross-linking degree of wheat gluten network

The degree of network cross-linking of wheat gluten-based materials was evaluated through the determination of the sodium dodecyl sulphate (SDS)-insoluble protein fraction (F_i) according to Domenek et al. [42]. Ground samples (160 mg) were stirred for 80 min at 60 °C into 20 mL 0.1 M of sodium phosphate buffer (pH 6.9) containing 1% SDS and subsequently centrifuged at 18,000 rpm for 30 min. The supernatant contained the SDS-soluble protein fraction (F_s). The SDS-insoluble protein fraction (F_i) was extracted with 5 mL of SDS-phosphate buffer containing 20 mmol L^{-1} dithioerythriol (DTE) under stirring for 60 min at 60 °C, then tip sonicated for 3 min and finally centrifuged 30 min at 18,000 rpm). 500 μL of the resulting supernatant was mixed with 500 μL of SDS-phosphate buffer containing 40 mmol L^{-1} iodoacetamide (IAM), (a sulfhydryl-reactive alkylating agent) used to block reduced cysteine residues. Both F_s and F_i extracts were submitted to size-exclusion HPLC. F_i was expressed in percent as the ratio of the SDS insoluble protein fraction on the total protein fraction ($F_i + F_s$).

2.5.2. Differential scanning calorimetry (DSC)

Differential scanning calorimetry was used to measure the glass transition temperature (T_g) of wheat gluten-based materials. Ground samples (around 12 mg) were placed in open aluminium pans (Tzero pan, TA Instruments New Castle, USA) and stored at a relative humidity of 75.3% over a saturated salt solution of NaCl. After equilibration, pans were immediately and hermetically sealed. Measurements were done with a thermo-modulated calorimeter (Q200 modulated DSC, TA Instruments, New Castle, USA). Each sample was heated from −40 to 130 °C at a heating rate of 3 °C min^{-1}. The period and the amplitude of modulation were respectively 100 s and 0.796 °C. The glass–rubber transition was characterized by the temperature at the inflexion point, corresponding to the temperature at which the differential heat flow was maximum. T_g values were measured in triplicate.

2.5.3. Wide angle X-ray scattering analysis (WAXS)

Ground samples and pristine nanoclays were characterized by wide angle X-ray scattering analysis at room temperature and relative humidity. Experiments were performed using a PHILIPS X'Pert MPD diffractometer (diffractometer $\theta - 2\theta$) with an X'celerator detector and a nickel filter operating at 40 kV and 20 mA with a Cu Kα radiation (λ = 1.5418 Å). The spectra were recorded between 2° and 25° using a scan speed of 0.035368° s^{-1} and a step size of 0.0334226°.

2.5.4. Transmission electron microscopy (TEM)

Materials were initially fixed in glutaraldehyde 2.5% (v/v), dehydrated in an ethanol gradient, then impregnated in propylene oxide and finally embedded in epoxy resin epon-812 substitute, (Electron Microscopy Science, England). After three days of incubation at 60 °C, ultra-thin sections of 70 nm were cut with an ultramicrotome diamond and mounted on 100 mesh grids covered by a colodion film. Samples were examined with a Jeol JEM-1200EX II TEM (Jeol Ltd., Tokyo, Japan) using magnifications from 10 to 100 K.

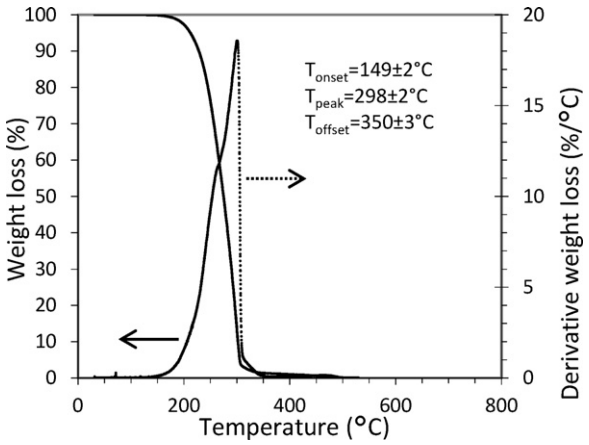

Fig. 1. Thermogravimetric analysis of ethofumesate under air flow.

2.6. Ethofumesate release kinetics in water

Appropriate amounts of granulates, corresponding to 16 mg of ethofumesate, were added to 0.8 L of deionised water with 0.2% (w/v) of sodium azide (to prevent microbial growth) in closed glass bottles of 1 L. Bottles were placed under magnetic stirring (200 rpm). At selected times, from 0 to 15 days, samples (500 μL) were taken, then passed through nylon filters (0.45 μm) and the amount of ethofumesate was analysed by HPLC. The same experiments were conducted with the commercial formulation (Tramat) used as control. Experiments were conducted at 8, 25 and 40 °C. Tests were performed in triplicate. All data were considered for data analysis whereas average values were used for plotting.

3. Ethofumesate analysis

Ethofumesate analysis was performed by HPLC using an Elite Lachrom-2400 UV/L chromatograph (VWR, France) coupled with a UV–vis 2420 detector. The following conditions were used: acetonitrile/water 70/30 eluent mixture at a flow rate of 0.7 mL min^{-1}, C18 nucleosil column (250 mm length × 4.9 mm i.d.) (Grace, France), 20 μL injection volume and UV detection at 280 nm at room temperature. External calibration curves with standard solutions were used in the calculations between 10 and 140 μM in water and between 10 and 2100 μM in water/ethanol (75/25).

4. Results and discussion

4.1. General characteristics of controlled release formulations

Morphological characteristics and ethofumesate content of wheat gluten-based controlled release granulates are shown in Table 1. Depending on the granulate formulation, the ethofumesate content ranged between 0.19 and 0.28 wt%, which can be considered as acceptable if compared to the targeted value (0.2 wt%). This also indicated that ethofumesate was compatible with the processing conditions required for the extrusion of wheat gluten (80 °C, 110 rpm). This result was expected if taking into account the degradation temperature of ethofumesate evidenced by TGA experiments (Fig. 1). Indeed, TGA curves showed that ethofumesate is a thermally stable chemical since the onset temperature of thermal degradation was around 150 °C, with a maximum degradation rate at about 300 °C. It is worth noting that such herbicide contents were in accordance with the required amount commonly used in

Table 1
Characteristics of wheat gluten-based granulates: morphological parameters (radius (r), thickness ($2l$), dry weight) and ethofumesate content.

	r (10^{-3} m)	$2l$ (10^{-3} m)	Dry weight (10^{-3} g)	Ethofumesate content (g 100 g^{-1})
WG–E	2.73 (±0.21)	1.10 (±0.07)	56.2 (±2)	0.26 (±0.03)
WG–HPS–E	2.42 (±0.07)	1.23 (±0.04)	51.0 (±0.3)	0.28 (±0.05)
WG–C30B–E	2.57 (±0.17)	1.12 (±0.12)	50.6 (±4)	0.19 (±0.02)
WG–D72T–E	2.80 (±0.17)	1.18 (±0.07)	61.6 (±2)	0.24 (±0.02)

Europe for agricultural applications. Indeed, the maximum application rate authorized (1 kg ha^{-1} per 3 years) would be reached by spreading around 500 kg of granulates per hectare (i.e., around 1000 granulates per m^2).

4.2. Influence of ethofumesate on the polymer network structure

The macromolecular structure of wheat gluten-based materials has been investigated through the evaluation of the degree of covalent cross-linking between protein chains, as revealed by the fraction of SDS-insoluble proteins (F_i) [42,43]. The extrusion process led to an increase of the F_i value from 9% (raw powder) to 28–33% depending on the formulation of wheat gluten-based materials (Fig. 2). This increase was due to the thermo-mechanical energy generated during the extrusion process as previously observed [35]. The presence of nanoclays had no influence on F_i values except in the presence of HPS. Indeed, for materials filled with the unmodified MMT, a slightly higher value was obtained, as reported in a previous work dealing with materials processed in the same conditions [35]. An anti-plasticisation effect of this hydrophilic unmodified MMT (HPS), resulting in a higher temperature at the core of the product during extrusion process, has been proposed to explain this result [35].

The F_i values obtained in the presence of ethofumesate were close to these previously obtained without ethofumesate (Fig. 2) leading to suggest that this active compound did not strongly affect the degree of cross-linking of the gluten network. However, in the case of materials filled with unmodified MMT (WG–HPS), a small but significant decrease in F_i value was noted indicating that the degree of cross-linking was reduced if compared to WG–HPS material without ethofumesate. As previously reported by Chevillard et al. [35], a decrease in F_i could be ascribed to a decrease of the melt viscosity during the extrusion process due to a plasticizing effect. In the present study, the plasticizing effect could be thus attributed to ethofumesate.

DSC measurements have been carried out to show how the presence of nanoclays and/or ethofumesate can affect the glass transition temperature of wheat gluten-based materials. This method would enable to evidence the potential establishment of interactions between the different components, which were expected to affect the polymer segmental motion at the interface. As shown in Fig. 3, the introduction of HPS in the WG matrix resulted in an increase of T_g which has been previously ascribed to a great affinity between these two hydrophilic components [35]. In the case of organically modified MMT (C30B and D72T), T_g values remained unchanged indicating that the protein chain mobility was not affected by the presence of these two hydrophobic fillers. Thus, it could be supposed that no specific interactions would be established between wheat gluten and organically modified MMT.

The presence of ethofumesate had no effect on the glass transition temperature of the unfilled material (Fig. 3). This suggested a low affinity of ethofumesate for wheat gluten since this pesticide was unable to affect the protein chain mobility at the very low pesticide concentration used in the formulation (0.2 wt%). Contrarily, in the case of materials filled with MMT, the polymer structure was affected by the presence of ethofumesate. In the case of HPS, ethofumesate induced a reduction of T_g from 47.8 (WG–HPS) to 45.4 °C (WG–HPS–E) indicating that the presence of ethofumesate would partially restore the loss of mobility induced by HPS. Based on the low affinity of ethofumesate for both wheat gluten (explained above) and HPS (already demonstrated in a previous work [14]), we assume that ethofumesate introduced in WG–HPS system would have no other possibility than interacting with itself and thus leading to the formation of clusters. As clusters, ethofumesate might act as a plasticizer inducing an increase of free volumes in the polymer matrix. This assumption was consistent with the small decrease in F_i values reported above.

For materials filled with organically modified MMT, a small increase in T_g was observed in the presence of ethofumesate (+1.5 °C for C30B and +2.3 °C for D72T) (Fig. 3). This change could be

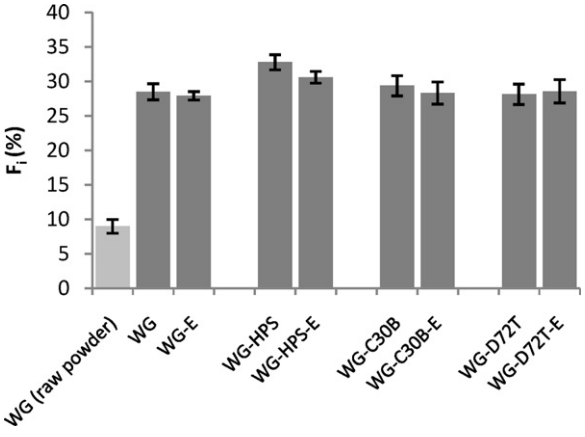

Fig. 2. F_i values of wheat gluten raw powder* and corresponding wheat gluten-based materials: unfilled material (WG*), unfilled material containing ethofumesate (WG–E), materials filled with unmodified MMT (WG–HPS*) or organically modified MMT (WG–C30B*, WG–D72T), and materials containing both ethofumesate and MMT (WG–HPS–E, WG–C30B–E, WG–D72T)
*Data obtained from [35].

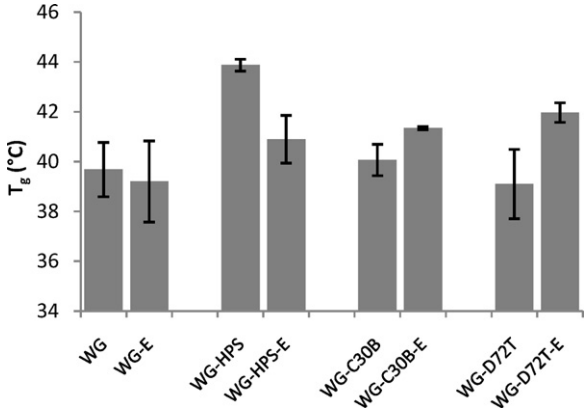

Fig. 3. Effect of wheat gluten-based materials formulation on the glass transition temperature (T_g): unfilled material (WG*), unfilled material containing ethofumesate (WG–E), materials filled with unmodified MMT (WG–HPS*) or organically modified MMT (WG–C30B*, WG–D72T), and materials containing both ethofumesate and MMT (WG–HPS–E, WG–C30B–E, WG–D72T–E).
*Data obtained from [35].

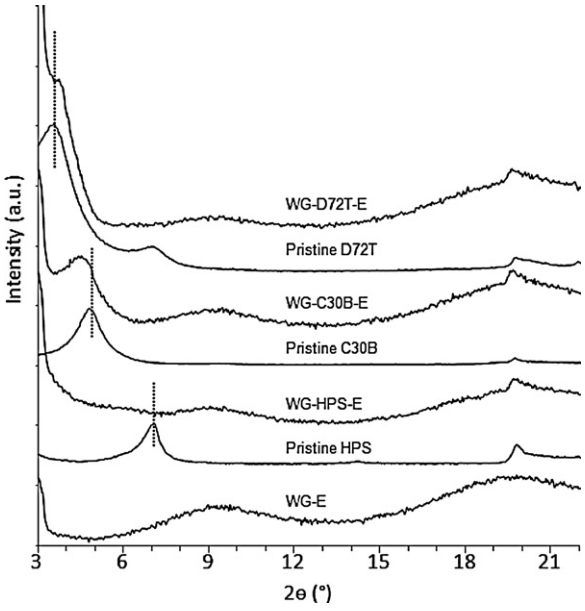

Fig. 4. Wide angle X-ray diffractogramms of pristine MMT (HPS, C30B and D72T), unfilled wheat gluten-based material containing ethofumesate (WG–E), and wheat gluten-based materials filled with unmodified MMT (WG–HPS–E) and organically modified MMMT (WG–C30B–E and WG–D72T–E).

interpreted as a reduction in the protein chain mobility induced by the concomitant presence of ethofumesate and OMMT. Taking into account the low affinity of wheat gluten for both OMMT and ethofumesate, we assume that in that case, wheat gluten in WG–OMMT systems would have no other possibility than interacting with itself and thus leading to a reduction of free volumes. This effect was even more likely to occur since the affinity of ethofumesate for OMMT was very high, as already underlined in a previous work [14].

4.3. Influence of ethofumesate on the wheat gluten/MMT nanocomposite structure

The influence of ethofumesate on the structure of wheat gluten-based materials at the nanometric scale was evaluated using WAXS analysis (Fig. 4) combined with TEM observations (Fig. 5). The unfilled matrix containing ethofumesate (WG–E) displayed a typical amorphous structure characterized by two very broad peaks centred around $2\theta = 8^\circ$ and $2\theta = 20^\circ$ on WAXS patterns (Fig. 4).

The WAXS pattern of the pristine HPS was characterized by a diffraction peak around $2\theta = 7^\circ$, corresponding to a basal interlayer spacing value d_{001} of 12.7 Å (Fig. 4). The introduction of HPS and ethofumesate in the wheat gluten matrix (WG–HPS–E) resulted in the disappearance of this peak. This could be interpreted as a good dispersion/exfoliation of the layered silicates within the matrix. Indeed, the presence of a peak around 20° ascribed to the crystallographic planes of the MMT demonstrated that the WAXS analysis was sufficiently sensitive to detect the presence of MMT (5 wt%) in this material. This result was supported by TEM observations showing that such materials displayed a well intercalated-exfoliated nanocomposite structure since almost all nanoclays appeared well dispersed (Fig. 5). A similar nanocomposite structure has already been obtained for materials processed in the same conditions but without ethofumesate [35]. This led to conclude that the presence of ethofumesate, even as clusters, would not influence the exfoliation level of unmodified MMT.

In the presence of the less hydrophobic organically modified MMT and ethofumesate (WG–C30B–E), the peak characteristic of the pristine clay was slightly shifted from $2\theta = 4.83^\circ$ ($d_{001} = 18.31$ Å) to $2\theta = 4.66^\circ$ ($d_{001} = 19.0$ Å), indicating that C30B nanoclays were not exfoliated but only partially intercalated (Fig. 4). Since it was shown in a previous study that in the absence of ethofumesate this peak was also shifted to $2\theta = 4.60^\circ$ ($d_{001} = 19.2$ Å) [35], it could be deduced that this intercalation, caused by partial penetration of the protein chain in the interlayer, was not perturbed by the presence of ethofumesate in the gallery. This hypothesis was in agreement with WAXS results previously obtained for C30B–ethofumesate complexes, showing that the interlayer distance of C30B was not affected by the presence of ethofumesate within the gallery [14].

In the presence of the most hydrophobic MMT and ethofumesate (WG–D72T–E), the diffraction peak characteristic of the pristine D72T ($d_{001} = 24.4$ Å), remained unchanged. Nevertheless, a potential increase of the interlayer distance would be difficult to evidence by WAXS since angle values of pristine D72T were very low.

Confirming WAXS results obtained for materials filled with organically modified MMT (C30B and D72T), TEM analyses demonstrated that a microcomposite structure was achieved in both cases. Indeed, TEM pictures were characterized by the presence of huge agglomerates of clays (micrometer sized) and very few dispersed particles (Fig. 5).As previously highlighted by Chevillard et al. [35], the chemical surface properties of the layered silicates appeared as a key parameter to reach a well-exfoliated nanocomposite structure. HPS appeared as the most suitable to be dispersed in the wheat gluten matrix due to the establishment of hydrogen bondings between the two components. On the contrary, the use of organically modified MMT such as C30B or D72T did not seem suitable to achieve a nanocomposite structure. The very hydrophobic nature of D72T led to very poor compatibility with wheat gluten and thus to a non-exfoliated structure in spite of its very high interlayer distance. Although C30B displayed a certain hydrophilicity (OH groups present on the interlayer cation) and a higher interlayer distance than HPS, it seems that the hydrophobic character of this clay dominated, leading to a poor compatibility with wheat gluten. Finally, it is worth noting that, whatever the type of MMT, similar structures at the nanometric scale were obtained for wheat gluten-based materials processed in the same conditions but without ethofumesate [35], leading to conclude that the presence of ethofumesate (0.2 wt%) did not affect the nanostructure, i.e., the dispersion and exfoliation level of nanoclays within the matrix.

4.4. How formulation influences ethofumesate release in water

4.4.1. Release modelling

All wheat gluten-based formulations displayed slow released properties if compared to the commercial formulation (Tramat® F) since all release values were lower than the commercial formulation (Fig. 6). Ethofumesate release data were not modelled by applying the commonly used empirical equation proposed by Rigter and Peppas [44]. Indeed, we proposed a more elaborated model based on Fick's second law taking into account granulate geometry, strong stirring and finite volume of the solution. In these conditions, the external mass transfer coefficient could be neglected while the partition coefficient between the polymer (wheat gluten-based materials) and the liquid (water) ($K_{pol/liq}$) could not. The solution of Fick's second law for diffusion from a finite cylinder of diameter $2r$ and height $2l$ immersed in a stirred solution of finite volume V_l was obtained by the superposition of the analytical solution for an infinite cylinder of diameter $2r$ (Eq. (1)) [45] and that for an infinite slab of thickness $2l$ (Eq. (3)) [45,46]:

$$\psi_r = 1 - \sum_{n=1}^{\infty} \frac{4\alpha(1+\alpha)}{4 + 4\alpha + \alpha^2 q_n^2} \exp\left(-\frac{Dq_n^2}{a^2}\right) \quad (1)$$

where $\alpha = (V_l)/(V_p)K_{pol/liq}$ with $V_p = h\pi r^2$ represents the volume of polymer and $K_{pol/liq}$ the partition coefficient of the migrant in the system between the polymer and the solution,

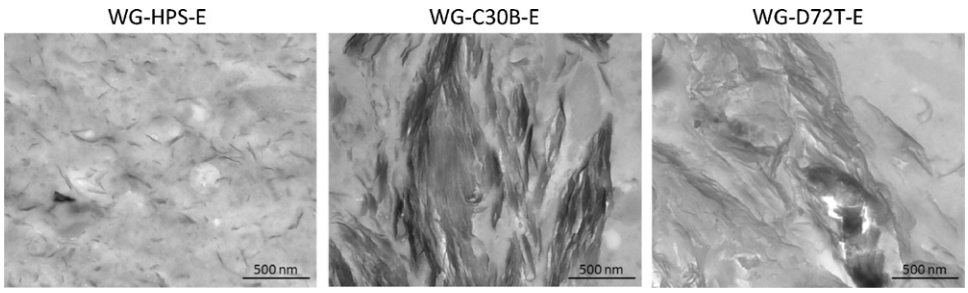

Fig. 5. TEM pictures of wheat gluten-based materials containing ethofumesate filled with unmodified MMT (WG–HPS–E) and organically modified MMMT (WG–C30B–E and WG–D72T–E).

which can be assumed as constant for law concentrations: $K_{pol/liq} = C_{polymer,\infty}/C_{liquid,\infty}$. In Eq. (1), q_n are the positive non-zero roots of:

$$\alpha q_n J_0(q_n) + J_1(q_n) = 0 \quad (2)$$

where $J_0(x)$ an $J1(x)$ are the Bessel function of order zero and first order respectively. Roots of Eq. (2) are tabulated in tables of Bessel functions [45].

$$\psi_z = 1 - \sum_{n=1}^{\infty} \frac{2\alpha + (1+\alpha)}{(1+\alpha+\alpha^2 p_n^2)} \exp\left(-\frac{p_n^2}{l^2} Dt\right) \quad (3)$$

where p_n are the non-zero positive roots of $\tan p_n = \alpha p_n$ given in Crank [45].

In Eqs. (1) and (3), ψ_r and ψ_z are the quantities of ethofumesate which go out of the theoretical infinite cylinder and infinite plane sheet at time t to the corresponding quantity after infinite time and D is the effective ethofumesate diffusivity. The quantity of ethofumesate going out of the finite cylinder at time t, ψ_t is then calculated as follows:

$$\psi_t = (\psi_r)(\psi_z) \quad (4)$$

In this approach, the swelling of the materials was neglected. Therefore, the diffusivities identified were considered as apparent diffusivity values called (D_{app}). Simulations of ethofumesate release were performed using equations 1, 3 and 4 programmed on MATLAB® software (The Mathworks Inc., Natick, MA, USA). Theoretical release kinetics were calculated vs time with initial conditions reported in Table 1 and partition coefficient values ($K_{pol/liq}$) calculated at equilibrium (Table 2). D_{app} was identified from the experimental curve by minimizing the root mean square deviations

$$\mathrm{RMSE} = \sqrt{\frac{(\hat{y} - y)^2}{N - p}} \quad (5)$$

between simulated and experimental results using the Levenberg–Marquardt procedure [47] via a dedicated routine "lsqnonlin" developed in MATLAB® (Table 3). In Eq. (5), $\hat{y}$ and y represent experimental and predicted values respectively, N is the number of experimental measurements and p is the number of estimated model parameters.

This model allowed to investigate, by an approach as realistic as possible, mechanisms involved in the release of active compounds by taking into account both kinetic (Dapp) and thermo-mechanical ($K_{pol/liq}$) parameters. The mechanistic model proposed fitted very well the experimental data for each temperature investigated (Fig. 6) as indicated by the low RMSE values obtained.

Table 2
Effect of material formulation on ethofumesate partition coefficients between the material and the aqueous medium ($K_{pol/liq}$) calculated at equilibrium from ethofumesate release experiments conducted at 8, 25 and 40 °C. Values between brackets are standard deviation.

	$K_{pol/liq}$		
	8 °C	25 °C	40 °C
WG–E	106 (±3)	69 (±7)	61 (±4)
WG–HPS–E	34 (±6)	24 (±3)	14 (±4)
WG–C30B–E	238 (±8)	158 (±13)	79 (±1)
WG–D72T–E	2774 (±138)	1286 (±118)	674 (±32)

4.5. Ethofumesate release in water at 25 °C

The quantity of ethofumesate released in water at 25 °C from wheat gluten-based materials was in the order WG–HPS > WG > WG–C30B > WG–D72T (Fig. 6b). If compared to the unfilled material, the addition of HPS surprisingly increased both (1) the total amount of ethofumesate released at the equilibrium (around 80% of release instead of 50%), also reflected by the thermodynamic parameter, $K_{pol/liq}$, 2.9-fold lower and (2) the ethofumesate diffusivity through the matrix (2.1-fold higher). Contrarily, the addition of organically modified MMT, C30B and D72T, reduced the total amount released at equilibrium (around 30% and 5% released, respectively) as well as the rate of release of

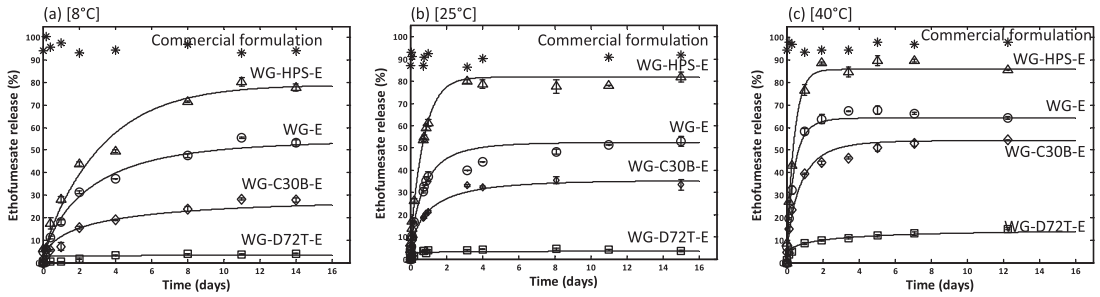

Fig. 6. Ethofumesate release kinetics obtained for the unfilled wheat gluten-based material (○), wheat gluten-based materials filled with HPS (Δ), C30B (◊) and D72T (□) and commercial formation (*) at 8 °C (a), 25 °C (b) and 40 °C. Symbols are experimental data points. Error bars represent standard deviation. Dot lines are fitting to the model. RMSE values were 0.04, 0.05, 0.10 and 0.51 at 8 °C; 0.05, 0.03, 0.04 and 0.39 at 25 °C; 0.04, 0.03, 0.05 0.15 at 40 °C for WG, WG–HPS, WG–C30B, WG–D72T respectively.

Table 3
Effect of material formulation on apparent diffusivity (D_{app}) of ethofumesate determined from release experiments conducted in water at 8, 25 and 40 °C, and corresponding activation energy (E_a). Values between brackets are 95% confidence intervals for diffusivity values and standard deviation for activation energy.

	$D_{app\ 8°C}$ [10^{-13} m^2 s^{-1}]	$D_{app\ 25°C}$ [10^{-13} m^2 s^{-1}]	$D_{app\ 40°C}$ [10^{-13} m^2 s^{-1}]	E_a [kJ mol^{-1}]	R^2
WG–E	11.3 (±1.3)	37.2 (±3.2)	101.9 (±13.2)	50 (±.9)	1.00
WG–HPS–E	20.7 (±2.5)	78.3 (±3.7)	144.6 (±15.5)	45 (±6.5)	0.98
WG–C30B–E	3.3 (±1.1)	13.8 (±1.3)	38.7 (±6.2)	57 (±1.6)	1.00
WG–D72T–E	0.1 (±0.9)	1.0 (±3.8)	2.5 (±2.3)	70 (±10.6)	0.98

ethofumesate (D_{app} 2.7- and 37-fold lower than for the unfilled material, for C30B and D72T, respectively).

Thus, in spite of its well exfoliated structure, the material filled with HPS delivered the pesticide faster and in greater quantity than the unfilled material suggesting that the tortuous pathway induced by the nanocomposite structure was ineffective to reduce ethofumesate diffusion. Another mechanism should be proposed to explain why ethofumesate release was favoured in that case. As explained above, the very low affinity of ethofumesate for both HPS and gluten was assumed to result in the formation of ethofumesate clusters. As a consequence, the diffusion process might be accelerated because of a higher affinity of ethofumesate for the solvent than for the matrix when filled with HPS.

Ethofumesate release kinetics from the material filled with D72T were characterized by D_{app} 37-fold lower and $K_{pol/liq}$ 19-fold higher than for the unfilled material (Tables 2 and 3). This was in agreement with the already demonstrated great affinity between this hydrophobic OMMT and ethofumesate, implying that a large amount of ethofumesate was irreversibly entrapped by the D72T interlayer cation [14]. It is worth noting that such a decrease in release rate and total amount has been obtained in spite of the bad dispersion of layered silicates. Since this bad dispersion resulted in clay aggregates in which ethofumesate might be entrapped, its diffusion would be delayed. Thus, it can be deduced that this release pattern was governed by sorption mechanisms between ethofumesate and D72T. Otherwise, this kind of formulation did not appear suitable for pesticide applications for two main reasons: (1) the amount released would not be sufficient to protect the crop, and (2) a too large amount would never be available since irreversibly entrapped. Concerning the material filled with C30B, an intermediate release pattern was obtained (Fig. 6b), in agreement with the already reported moderate affinity of this clay for ethofumesate if compared to D72T [14]. As observed above with D72T, it seems that ethofumesate/C30B interactions dominated release mechanisms since ethofumesate delivery was slowed down and limited in quantity, in spite of a bad dispersion of the layered silicates. This last formulation appeared as a more suitable support for slow release applications.

4.6. Effect of temperature on release pattern

Whatever the temperature (8, 25 or 40 °C), the quantity of ethofumesate released was still in the order WG–HPS > WG > WG–C30B > WG–D72T with a significant effect on the release pattern of ethofumesate (Fig. 6a–c). Raising the temperature from 8 to 40 °C caused (1) a faster rate of release, as indicated by an increased D_{app} values and (2) a higher amount released at equilibrium, as evidenced by decreased $K_{pol/liq}$ values (Tables 2 and 3). The temperature-induced variation of D_{app} ranged from 7% to 25% in the order WG–HPS < WG < WG–C30B < WG–D72T, while for $K_{pol/liq}$, the variation ranged from 1.8% to 4.1% in the order WG < WG–HPS < WG–C30B < WG–D72T.

The diffusion of a chemical through a polymer matrix is generally well described by the Arrhenius equation (Eq. (6)), where the activation energy of diffusion (E_a) is the energy required to produce an opening between the polymer chains that is large enough for a chemical molecule to move through [48]. Thus, in order to further explore the effect of temperature on the ethofumesate diffusion kinetics, apparent diffusivity values (D_{app}) were fitted using the following Arrhenius equation:

$$D_{app} = D_0 \exp\left(\frac{-E_a}{RT}\right) \quad (6)$$

where D_0 is the pre-exponential factor of diffusion, R is the ideal gas constant, and T is the temperature in Kelvin. As expected, E_a values were found in the order WG–HPS < WG < WG–C30B < WG–D72T (Table 3) indicating that more energy would be required for ethofumesate to diffuse through the material filled with the most apolar MMT (D72T). Conversely, less energy was required for ethofumesate to diffuse through the material filled with the most HPS. The temperature dependency of ethofumesate diffusivity could be explained by the temperature effect on the solubility and the molecular mobility of the diffusing molecule in the material, and the nature of interactions at the interface between ethofumesate and clay surfaces, as already observed in various systems [49–52]. In the present study, the increase of E_a while increasing the hydrophobic character of the MMT confirmed the hydrophobic nature of interactions established between ethofumesate and layered silicates. Indeed, hydrophobic interactions are generally known to be favoured while increasing temperature.

5. Conclusion

Slow release formulations of a model pesticide (ethofumesate) have been successfully obtained by associating an agropolymer matrix (wheat gluten) and montmorillonites. Results showed that the affinity between layered silicate and wheat gluten was the key parameter to achieve a well-exfoliated nanocomposite structure. Nevertheless, the tortuous pathway resulting from this nanocomposite structure had no significant effect on the slowdown of ethofumesate release in water. Actually, the entrapment of ethofumesate in clay aggregates appeared as more effective to reduce its diffusivity through the material. Finally, we have shown that the release mechanisms were governed by ethofumesate/MMT interactions and not by wheat gluten/MMT interactions. Indeed, due to the hydrophobic nature of ethofumesate, the slow release effect was favoured in the presence of hydrophobic clays.

The mechanistic approach proposed in the present study appeared suitable, not only to fit experimental data, but also to identify quantitative parameters such as apparent diffusivity. Such knowledge would enable to develop integrative models taking into account ethofumesate diffusivity both in the material and the soil. The perspectives of this work are to predict the pesticide fate once the formulations are applied on field. The objective would consist in developing effective controlled release systems by adjusting (i) the material size and (ii) the formulation (ethofumesate content, type and amount of nanoclay) to the needs of selected crops.

Acknowledgements

ADEME (Agence de l'Environnement et de la Maîtrise de l'Energie, France) is acknowledged for its financial support (reference no. 0701C0035 DBIO). The authors thank Bayer Crop

Science (France) for supplying technical ethofumesate and gratefully acknowledge Didier Cot (IEM, Montpellier) and Chantal Cazevieille (CRIC, Montpellier) for MEB and TEM observations.

References

[1] I. Ravier, E. Haouisee, M. Clement, R. Seux, O. Briand, Field experiments for the evaluation of pesticide spray-drift on arable crops, Pest Manag. Sci. 61 (2005) 728–736.
[2] M.G. Mogul, H. Akin, N. Hasirci, D.J. Trantolo, J.D. Gresser, D.L. Wise, Controlled release of biologically active agents for purposes of agricultural crop management, Resour. Conserv. Recycl. 16 (1996) 289–320.
[3] M. Bahadir, Safe formulations of agrochemicals, Chemosphere 16 (1987) 615–621.
[4] Z. Gerstl, A. Nasser, U. Mingelgrin, Controlled release of pesticides into water from clay-polymer formulations, J. Agric. Food Chem. 46 (1998) 3803–3809.
[5] R. Celis, M.C. Hermosin, M.J. Carrizosa, J. Cornejo, Inorganic and organic clays as carriers for controlled release of the herbicide hexazinone, J. Agric. Food Chem. 50 (2002) 2324–2330.
[6] F. Bruna, I. Pavlovic, R. Celis, C. Barriga, J. Cornejo, M.A. Ulibarri, Organohydrotalcites as novel supports for the slow release of the herbicide terbuthylazine, Appl. Clay Sci. 42 (2008) 194–200.
[7] M. Fernandez-Perez, M. Villafranca-Sanchez, E. Gonzalez-Pradas, F. Flores-Cespedes, Controlled release of diuron from an alginate–bentonite formulation: water release kinetics and soil mobility study, J. Agric. Food Chem. 47 (1999) 791–798.
[8] O.D. Dailey, Volatilization of alachlor from polymeric formulations, J. Agric. Food Chem. 52 (2004) 6742–6746.
[9] L. Cornejo, R. Celis, C. Domínguez, M.C. Hermosín, J. Cornejo, Use of modified montmorillonites to reduce herbicide leaching in sports turf surfaces: laboratory and field experiments, Appl. Clay Sci. 42 (2008) 284–291.
[10] R. Celis, C. Trigo, G. Facenda, M. Hermosin, J. Cornejo, Selective modification of clay minerals for the adsorption of herbicides widely used in olive groves, J. Agric. Food Chem. 55 (2007) 6650–6658.
[11] M. Cruz-Guzman, R. Celis, M.C. Hermosin, W.C. Koskinen, J. Cornejo, Adsorption of pesticides from water by functionalized organobentonites, J. Agric. Food Chem. 53 (2005) 7502–7511.
[12] M.C. Hermosin, M.J. Calderon, J.P. Aguer, J. Cornejo, Organoclays for controlled release of the herbicide fenuron, Pest Manag. Sci. 57 (2001) 803–809.
[13] M.J. Carrizosa, M.J. Calderon, M.C. Hermosin, J. Cornejo, Organosmectites as sorbent and carrier of the herbicide bentazone, in: 2nd Iberian Congress on Environmental Contamination and Toxicology, Basque Country, Spain, 1998, pp. 285–293.
[14] A. Chevillard, H. Angellier-Coussy, S. Peyron, N. Gontard, E. Gastaldi, Investigating ethofumesate – clay interactions for pesticide controlled release, Soil Sci. Soc. Am. J., doi:10.2136/sssaj201, in press.
[15] D.J. Park, W.R. Jackson, I.R. McKinnon, R. Marshall, Controlled release of pesticides from microparticles, in: H.B. Scher (Ed.), Controlled-release delivery systems for pesticides, Dekker, New York, 1999, pp. 89–136.
[16] S.A. Agnihotri, T.M. Aminabhavi, Controlled release of clozapine through chitosan microparticles prepared by a novel method, J. Control. Release 96 (2004) 245–259.
[17] M.A. Teixeira, W.J. Paterson, E.J. Dunn, Q. Li, B.K. Hunter, M.F.A. Goosen, Assessment of chitosan gels for the controlled release of agrochemicals, Ind. Eng. Chem. Res. 29 (1990) 1205–1209.
[18] J. Zhao, R.M. Wilkins, Low molecular weight polylactic acid as a matrix for the delayed release of pesticides, J. Agric. Food Chem. 53 (2005) 4076–4082.
[19] Y.S. Cao, L. Huang, J.X. Chen, J. Liang, S.Y. Long, Y.T. Lu, Development of a controlled release formulation based on a starch matrix system, Int. J. Pharm. 298 (2005) 108–116.
[20] D. Trimnell, B.S. Shasha, Controlled release formulations of atrazine in starch for potential reduction of groundwater pollution, J. Control. Release 12 (1990) 251–256.
[21] B. Singh, D.K. Sharma, R. Kumar, A. Gupta, Development of a new controlled pesticide delivery system based on neem leaf powder, J. Hazard. Mater. 177 (2010) 290–299.
[22] B. Singh, D.K. Sharma, A. Gupta, A study towards release dynamics of thiram fungicide from starch–alginate beads to control environmental and health hazards, J. Hazard. Mater. 161 (2009) 208–216.
[23] A.R. Kulkarni, K.S. Soppimath, T.M. Aminabhavi, A.M. Dave, M.H. Mehta, Glutaraldehyde crosslinked sodium alginate beads containing liquid pesticide for soil application, J. Control. Release 63 (2000) 97–105.
[24] A.B. Pepperman, J.-C.W. Kuan, Controlled release formulations of alachlor based on calcium alginate, J. Control. Release 34 (1995) 17–23.
[25] A. Roy, J. Bajpai, A.K. Bajpai, Development of calcium alginate–gelatin based microspheres for controlled release of endosulfan as a model pesticide, Indian J. Chem. Technol. 16 (2009) 388–395.
[26] A. Roy, A.K. Bajpai, J. Bajpai, Designing swellable beads of alginate and gelatin for controlled release of pesticide (cypermethrin), J. Macromol. Sci. A 46 (2009) 847–859.
[27] F.M. Pereira, A.R. Goncalves, A. Ferraz, F.T. Silva, S.C. Oliveira, Modeling of 2,4-dichlorophenoxyacetic acid controlled-release kinetics from lignin-based formulations, Appl. Biochem. Biotechnol. 98 (2002) 101–107.
[28] M. Fernandez-Perez, Controlled release systems to prevent the agro-environmental pollution derived from pesticide use, J. Environ. Sci. Health B 42 (2007) 857–862.
[29] M. Fernandez-Perez, F.J. Garrido-Herrera, E. Gonzalez-Pradas, M. Villafranca-Sanchez, F. Flores-Cespedes, Lignin and ethylcellulose as polymers in controlled release formulations of urea, J. Appl. Polym. Sci. 108 (2008) 3796–3803.
[30] F.J. Garrido-Herrera, I. Daza-Fernández, E. González-Pradas, M. Fernández-Pérez, Lignin-based formulations to prevent pesticides pollution, J. Hazard. Mater. 168 (2009) 220–225.
[31] D. Gómez-Martínez, P. Partal, I. Martínez, C. Gallegos, Rheological behaviour and physical properties of controlled-release gluten-based bioplastics, Bioresour. Technol. 100 (2009) 1828–1832.
[32] L. Andreani, R. Cercená, B.G.Z. Ramos, V. Soldi, Development and characterization of wheat gluten microspheres for use in a controlled release system, Mater. Sci. Eng. C 29 (2009) 524–531.
[33] A. Redl, M.H. Morel, J. Bonicel, B. Vergnes, S. Guilbert, Extrusion of wheat gluten plasticized with glycerol: influence of process conditions on flow behavior, rheological properties, and molecular size distribution, Cereal Chem. 76 (1999) 361–370.
[34] S. Domenek, P. Feuilloley, J. Gratraud, M.-H. Morel, S. Guilbert, Biodegradability of wheat gluten based bioplastics, Chemosphere 54 (2004) 551–559.
[35] A. Chevillard, H. Angellier-Coussy, B. Cuq, V. Guillard, G. César, N. Gontard, E. Gastaldi, How the biodegradability of wheat gluten based agromaterial can be modulated by adding nanoclays, Polym. Degrad. Stabil. 96 (2011) 2088–2097.
[36] T. Undabeytia, F. Sopena, T. Sanchez-Verdejo, J. Villaverde, S. Nir, E. Morillo, C. Maqueda, Performance of slow-release formulations of alachlor, Soil Sci. Soc. Am. J. 74 (2010) 898–905.
[37] Q. Wang, X. Xie, X. Zhang, J. Zhang, A. Wang, Preparation and swelling properties of pH-sensitive composite hydrogel beads based on chitosan-g-poly (acrylic acid)/vermiculite and sodium alginate for diclofenac controlled release, Int. J. Biol. Macromol. 46 (2010) 356–362.
[38] F.F. Cespedes, M.V. Sanchez, S.P. Garcia, M.F. Perez, Modifying sorbents in controlled release formulations to prevent herbicides pollution, Chemosphere 69 (2007) 785–794.
[39] B. Singh, D.K. Sharma, R. Kumar, A. Gupta, Controlled release of thiram from neem–alginate–clay based delivery systems to manage environmental and health hazards, Appl. Clay Sci. 47 (2010) 384–391.
[40] A. Sorrentino, M. Tortora, V. Vittoria, Diffusion behavior in polymer–clay nanocomposites, J. Polym. Sci. Polym. Phys. 44 (2006) 265–274.
[41] G. Choudalakis, A.D. Gotsis, Permeability of polymer/clay nanocomposites: a review, Eur. Polym. J. 45 (2009) 967–984.
[42] S. Domenek, M.-H.l.n. Morel, J. l. Bonicel, S.p. Guilbert, Polymerization kinetics of wheat gluten upon thermosetting. A mechanistic model, J. Agric. Food Chem. 50 (2002) 5947–5954.
[43] M.H. Morel, A. Redl, S. Guilbert, Mechanism of heat and shear mediated aggregation of wheat gluten protein upon mixing, Biomacromolecules 3 (2002) 488–497.
[44] P.L. Ritger, N.A. Peppas, A simple equation for description of solute release I. Fickian and non-fickian release from non-swellable devices in the form of slabs, spheres, cylinders or discs, J. Control. Release 5 (1987) 23–36.
[45] J. Crank, The Mathematics of Diffusion, Oxford University Press, 1976.
[46] E. Mascheroni, V. Guillard, F. Nalin, L. Mora, L. Piergiovanni, Diffusivity of propolis compounds in polylactic acid polymer for the development of anti-microbial packaging films, J. Food Eng. 98 (2010) 294–301.
[47] P.E. Gill, W. Murray, M.H. Wright, Practical Optimization, Academic Press, London, 1981.
[48] W. Limm, H.C. Hollifield, Modelling of additive diffusion in polyolefins, Food Addit. Contam. 13 (1996) 949–967.
[49] E.E. Perez, A.A. Carelli, G.H. Crapiste, Temperature-dependent diffusion coefficient of oil from different sunflower seeds during extraction with hexane, J. Food Eng. 105 (2011) 180–185.
[50] P. Suppakul, K. Sonneveld, S.W. Bigger, J. Miltz, Diffusion of linalool and methylchavicol from polyethylene-based antimicrobial packaging films, LWT Food Sci. Technol. 44 (2011) 1888–1893.
[51] V. Guillard, B. Broyart, C. Bonazzi, S. Guilbert, N. Gontard, Moisture diffusivity in sponge cake as related to porous structure evaluation and moisture content, J. Food Sci. 68 (2003) 555–562.
[52] S. Myint, W.R.W. Daud, A.B. Mohamad, A.A.H. Kadhum, Temperature-dependent diffusion coefficient of soluble substances during ethanol extraction of clove, J. Am. Oil Chem. Soc. 73 (1996) 603–610.